Theoretical analysis and an improvement method of the bias effect on the linearity of RF linear power amplifiers

Wu Tuo(吴拓)[1,†], Chen Hongyi(陈弘毅)[1], and Qian Dahong(钱大宏)[2]

(1 Institute of Microelectronics, Tsinghua University, Beijing 100084, China)

(2 Accel Semiconductor Corp, Shanghai 201203, China)

Abstract: Based on the Gummel–Poon model of BJT, the change of the DC bias as a function of the AC input signal in RF linear power amplifiers is theoretically derived, so that the linearity of different DC bias circuits can be interpreted and compared. According to the analysis results, a quantitative adaptive DC bias circuit is proposed, which can improve the linearity and efficiency. From the simulation and test results, we draw conclusions on how to improve the design of linear power amplifier.

Key words: bipolar; large-signal model; DC bias; linearity; adaptive bias

DOI: 10.1088/1674-4926/30/5/055002 **EEACC:** 1160; 1220

1. Introduction

Owing to its high power-efficiency, linear modulation is widely adopted in modern wireless communication systems, such as enhanced-data-rate Bluetooth and WLAN 802.11b/g. But the stringent requirement of linearity complicates the design of RF transceivers[1], especially the design of the power amplifier (PA) module in transmitters. A recently published work on PAs showed that the nonlinearity can be optimized by tuning the source/load impedance of the baseband and the 2nd harmonic frequency[2]. The traditional nonlinear analysis method using Volterra Series is usually based on a small-signal model of transistors[3], while it hardly describes the large-signal nonlinearity[4] for the omission of the DC offset with AC input. Reference [5] proposed a novel DC bias circuit to improve the linearity of RF PAs, and Reference [6] indicated qualitatively that the DC bias resistance can affect the nonlinearity. But so far no reports are available, which theoretically analyze the bias affection on the linearity of RF linear PAs. This paper derives the nonlinearity of conventional biased-linear RF PAs (Class A/AB) made using a bipolar process, and proposes a novel adaptive-current bias prototype to improve the maximum linear output power.

2. Theoretical analysis of the DC bias effect on the linearity of a linear bipolar PA

Figure 1 shows two commonly used DC bias circuits for linear bipolar PAs: regular bias and diode bias[5]. A voltage bias and a current bias ($I_{\rm Bias}$ = const, $R_{\rm Bias}$ = $+\infty$) can be combined to form a traditional regular bias (Fig. 1(a)). Figure 1(b) is the novel diode bias circuit proposed in Ref. [4].

2.1. Regular bias of an RF linear PA

2.1.1. Simplified large-signal equivalent circuit of a bipolar linear PA

Based on the Gummel–Poon model for bipolar transistors, Figure 2 shows the simplified large-signal equivalent circuit of a linear PA including source and load impedances. $C_{\rm couple}$ and $L_{\rm choke}$ are the DC blocking capacitor and the RF choke, respectively, the real values of which can be in series or in parallel with the source/load impedance ($Z_{\rm s}/Z_{\rm L}$). $Z_{\rm e}$ is due to the the emitter resistance and the bondwire inductor. $C_{\rm d}$ is the base diffusion capacitance, which is related to the forward transmit time τ and the collector current $i_{\rm C}$.

$$C_{\rm d} = \tau \frac{{\rm d}i_{\rm C}}{{\rm d}v_{\rm be}}. \tag{1}$$

$C_{\rm je}$ and $C_{\rm jc}$ are the junction capacitances of BE and BC, which are approximately constant compared to the nonlinear $C_{\rm d}$. The collector and base voltage-controlled current sources are respectively:

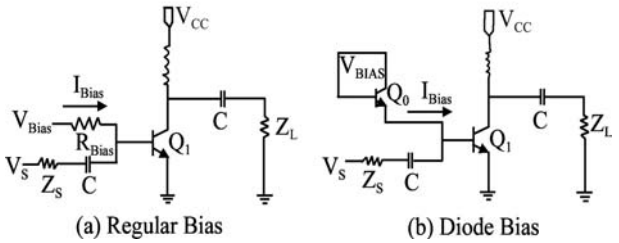

Fig. 1. Two different DC bias circuits.

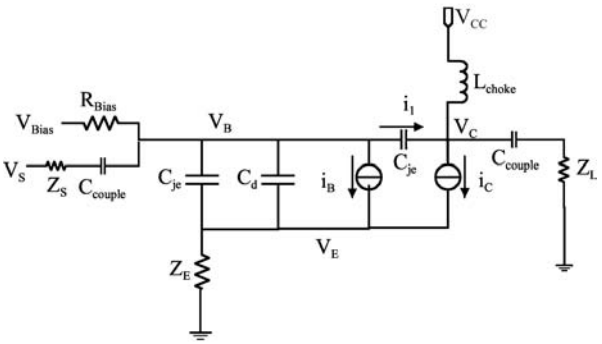

Fig. 2. Simplified large-signal equivalent model of a regular biased linear PA.

† Corresponding author. Email: wutuo@tsinghua.org.cn

Received 11 December 2008, revised manuscript received 17 January 2009

$$i_{\rm C} = I_{\rm S}\left(\exp\frac{v_{\rm BE}}{V_{\rm T}} - 1\right) = I_{\rm S}\left(\exp\frac{v_{\rm BE}+v_{\rm BE}}{V_{\rm T}} - 1\right) \approx I_0 \exp\frac{v_{\rm be}}{V_{\rm T}}, \quad (2)$$

$$i_{\rm B} \approx \frac{i_{\rm C}}{\beta} \approx \frac{I_0}{\beta}\exp\frac{v_{\rm be}}{v_{\rm T}}, \quad (3)$$

where $I_0 = I_{\rm S}\exp\dfrac{V_{\rm BE}}{V_{\rm T}}$, $V_{\rm BE}$ means the DC voltage, $v_{\rm be}$ means the AC voltage, $v_{\rm BE} = V_{\rm BE} + v_{\rm be}$.

2.1.2. Nonlinear AC analysis

As shown in Fig. 2, $|Z_{\rm s}|$ is usually much smaller than $R_{\rm Bias}$; so, the 3rd order nonlinear approximation equation of the AC analysis can be written as (see Appendix):

$$v_{\rm s} = B_1(s)\left(\frac{v_{\rm be}}{V_{\rm T}}\right) + B_2(s)\left(\frac{v_{\rm be}}{V_{\rm T}}\right)^2 + B_3(s)\left(\frac{v_{\rm be}}{V_{\rm T}}\right)^3, \quad (4)$$

where

$$B_1(s) = V_{\rm T} + I_0 Z_{\rm e} + \left[I_0\left(\frac{1}{\beta}+s\tau\right) + sC_{\rm je}V_{\rm T}\right](Z_{\rm s}+Z_{\rm e}) + \frac{sC_{\rm jc}Z_{\rm s}}{1+sC_{\rm jc}Z_{\rm L}}\left[\left(1+sC_{\rm je}Z_{\rm e}\right)V_{\rm T} + I_0\left(1+\frac{1}{\beta}+s\tau\right)Z_{\rm e} + I_0 Z_{\rm L}\right],$$

$$B_2(s) = \frac{I_0}{2}Z_{\rm e} + \frac{I_0}{2}\left(\frac{1}{\beta}+s\tau\right)(Z_{\rm s}+Z_{\rm e}) + \frac{I_0}{2}\frac{sC_{\rm jc}Z_{\rm s}}{1+sC_{\rm jc}Z_{\rm L}}\left[Z_{\rm L} + \left(1+\frac{1}{\beta}+s\tau\right)Z_{\rm e}\right],$$

$$B_3(s) = \frac{I_0}{6}Z_{\rm e} + \frac{I_0}{6}\left(\frac{1}{\beta}+s\tau\right)(Z_{\rm s}+Z_{\rm e}) + \frac{I_0}{6}\frac{sC_{\rm jc}Z_{\rm s}}{1+sC_{\rm jc}Z_{\rm L}}\left[Z_{\rm L} + \left(1+\frac{1}{\beta}+s\tau\right)Z_{\rm e}\right].$$

According to Volterra's theory[7],

$$\frac{v_{\rm be}}{V_{\rm T}} = C_1(s)\circ v_{\rm s} + C_2(s_1,s_2)\circ v_{\rm s}^2 + C_3(s_1,s_2,s_3)\circ v_{\rm s}^3, \quad (5)$$

where

$$C_1(s) = \frac{1}{B_1(s)},$$

$$C_2(s_1,s_2) = -C_1(s_1)C_1(s_2)B_2(s_1+s_2)C_1(s_1+s_2),$$

$$C_3(s_1,s_2,s_3) = -C_1(s_1)C_1(s_2)C_1(s_3)B_3(s_1+s_2+s_3)C_1(s_1+s_2+s_3) - 2\overline{C_1C_2}B_2(s_1+s_2+s_3)C_1(s_1+s_2+s_3).$$

2.1.3. DC analysis

An AC input would cause a DC offset due to an even-order nonlinearity. So, the DC equation can be written as (see Appendix)

$$V_{\rm T}\ln\frac{I_0}{I_{\rm s}} + I_0\frac{R_{\rm Bias}}{\beta} + I_0\frac{v_{\rm sm}^2}{4}|C_1(s)|^2\frac{R_{\rm Bias}}{\beta} - V_{\rm Bias} = 0. \quad (6)$$

This means that I_0 is related to $v_{\rm sm}$, $I_0 = I_0(v_{\rm sm})$.

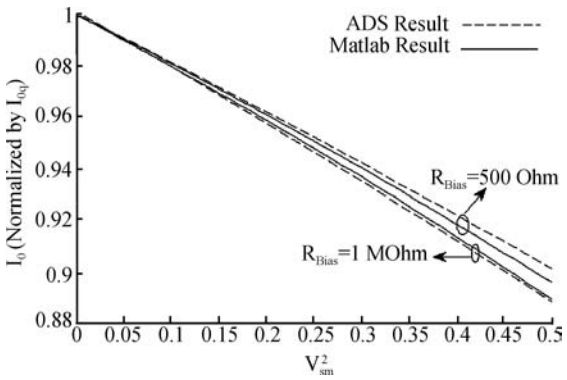

Fig. 3. Curves of the DC current I_0 versus $v_{\rm sm}$ and $R_{\rm Bias}$.

When $v_{\rm sm} = 0$, $I_0(0) = I_{0\rm q}$, Equation (6) can be rewritten as

$$V_{\rm T}\ln\frac{I_{0\rm q}}{I_{\rm s}} + I_{0\rm q}\frac{R_{\rm Bias}}{\beta} - V_{\rm Bias} = 0. \quad (7)$$

When subtracting Eq. (7) from Eq. (6) and using $\ln\frac{I_0}{I_{0\rm q}} \approx \frac{I_0-I_{0\rm q}}{I_{0\rm q}}$, we get

$$I_0 = \frac{I_{0\rm q}}{1+\dfrac{kv_{\rm sm}^2}{1+\dfrac{\beta V_{\rm T}}{I_{0\rm q}R_{\rm Bias}}}}, \quad (8)$$

where $k = \dfrac{|C_1(s)|^2}{4}$.

If the bias is an ideal current source, $R_{\rm Bias} = \infty$, so

$$I_0 \approx \frac{I_{0\rm q}}{1+kv_{\rm sm}^2} \approx I_{0\rm q}\left(1-kv_{\rm sm}^2\right). \quad (9)$$

So, I_0 would reduce with an increase of $v_{\rm sm}$ and $R_{\rm Bias}$. Using Eq. (8), more accurate curves can be calculated using ADS and MATLAB, as shown in Fig. 3.

2.1.4. IMR analysis

If the input is composed of two adjacent tones,

$$v_{\rm s} = \frac{v_{\rm sm}}{\sqrt{2}}(\cos\omega_1 t + \cos\omega_2 t) = \frac{v_{\rm sm}}{2\sqrt{2}}\left(e^{s_1 t} + e^{-s_1 t} + e^{s_2 t} + e^{-s_2 t}\right), \quad (10)$$

where $s_1 \approx s_2 \approx 2s_1 - s_2 \approx 2s_2 - s_1 \approx s$.

The 3rd inter-modulation ratio is[8](see Appendix):

$$|{\rm IMR3}| = \left|\frac{3}{4}\frac{F_3(s_1,s_1,-s_2)}{F_1(s_1)}\right|\left|\frac{v_{\rm sm}}{\sqrt{2}}\right|^2 = \frac{3|v_{\rm sm}|^2}{8}f_1(I_0), \quad (11)$$

where

$$f_1(I_0) = |C_1(s)|^2\left|\frac{E_3(s)}{E_1(s)} - C_1(s)B_3(s) + 2\overline{B_2C_1}\left[C_1(s)B_2(s) - \frac{E_2(s)}{E_1(s)}\right]\right|,$$

$$\overline{B_2C_1} = \frac{2B_2(0)C_1(0) + B_2(2s)C_1(2s)}{3}.$$

The function of $f_1(I_0)$ is complicated, but it could be plotted by using MATLAB, as shown in Fig. 4.

From Figs. 3 and 4, we can see that $f_1(I_0)$ will increase as $v_{\rm sm}$ increases, so that the 3rd order inter-modulation product (IMR3) would reduce compared to the standard results, which means the IMR3 is proportional to $|v_{\rm sm}|^2$. Simulation result by

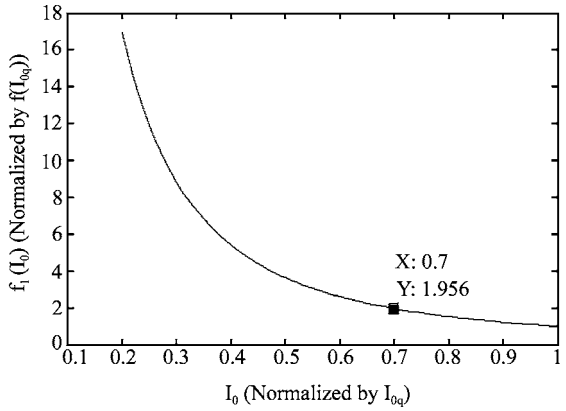

Fig. 4 Curve of $f_1(I_0)$ (Normalized).

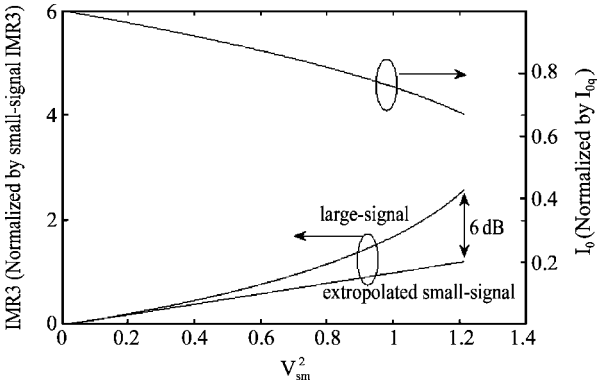

Fig. 5. AC-influence on the DC current I_0 and the IMR3 (normalized).

MATLAB shows that the IMR3 is 6 dB higher than the standard result when the DC current I_0 drops to 70% of the quiescent value.

2.1.5. Summary of the regular biased linear PA

Equation (8) indicates that a larger bias resistance would generate more nonlinearity. Thus, to gain a better linearity in the design of an RF linear PA, $R_{\rm Bias}$ should be chosen to be small, which, however, leads to a large leakage current in the bias branch. Another potential disadvantage of a small $R_{\rm Bias}$ is the temperature dependence of the bias current. The partial differential of Eq. (7) with respect to temperature (ignoring the temperature coefficients of $R_{\rm Bias}$ and $I_{\rm s}$) is given by:

$$\frac{\partial I_{0\rm q}}{\partial T} = -\ln\frac{I_{0\rm q}}{I_{\rm s}}\frac{I_{0\rm q}}{\left(\dfrac{I_{0\rm q}R_{\rm Bias}}{V_{\rm T}\beta}+1\right)T}. \tag{12}$$

Equation (12) shows that the differential of $I_{0\rm q}$ with respect to temperature is inversely proportional to $R_{\rm Bias}$.

2.2. Diode bias of a linear PA

2.2.1. AC analysis

Figure 6 shows the large-signal simplified equivalent circuit of a diode biased linear PA. Generally, the size of the diode is very small, which means that the AC resistance of the bias branch can be neglected in an AC analysis of the linear PA, so that the AC equations are equivalent to the equations of regular biased PAs.

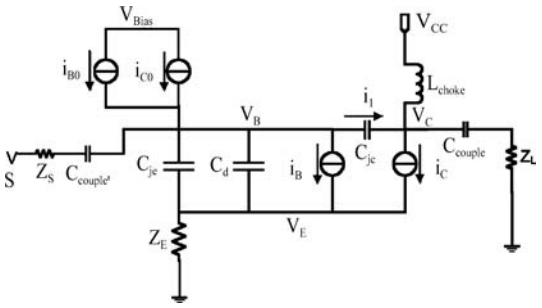

Fig. 6. Large-signal simplified equivalent circuit of a diode biased linear PA.

2.2.2. DC analysis

Contrary to a regular biased linear PA, the DC equation with input signal $v_{\rm sm} \neq 0$ is

$$V_{\rm T}\ln\frac{I_0}{I_{\rm s}}+\left(1+\frac{1}{\beta}\right)\left(I_0+I_0\frac{v_{\rm sm}^2}{4}|C_1(s)|^2\right)R_{\rm e} +V_{\rm T}\ln\frac{I_0+I_0\dfrac{v_{\rm sm}^2}{4}|C_1(s)|^2}{\beta\left(1+\dfrac{1}{\beta}\right)I_{\rm s0}}-V_{\rm Bias}=0. \tag{13}$$

When $v_{\rm sm}=0$, Equation (13) can be written as

$$V_{\rm T}\ln\frac{I_{0\rm q}}{I_{\rm s}}+\left(1+\frac{1}{\beta}\right)I_{0\rm q}R_{\rm e}+V_{\rm T}\ln\frac{I_{0\rm q}}{\beta\left(1+\dfrac{1}{\beta}\right)I_{\rm s0}}-V_{\rm Bias}=0. \tag{14}$$

When subtracting Eq. (14) from Eq. (13) and making the following approximation

$$\ln\frac{I_0}{I_{0\rm q}}\approx\frac{I_0-I_{0\rm q}}{I_{0\rm q}},\quad \ln\left(1+\frac{v_{\rm sm}^2}{4}|C_1(s)|^2\right)\approx\frac{v_{\rm sm}^2}{4}|C_1(s)|^2,$$

we can calculate the DC current:

$$I_0=\frac{(2-kv_{\rm sm}^2)V_{\rm T}+\left(1+\dfrac{1}{\beta}\right)I_{0\rm q}R_{\rm e}}{\dfrac{2V_{\rm T}}{I_{0\rm q}}+\left(1+\dfrac{1}{\beta}\right)(1+kv_{\rm sm}^2)R_{\rm e}}, \tag{15}$$

where $k=\dfrac{|C_1(s)|^2}{4}$.

Usually $R_{\rm e}\ll\dfrac{V_{\rm T}}{I_{0\rm q}}$, so

$$I_0\approx\left(1-\frac{kv_{\rm sm}^2}{2}\right)I_{0\rm q}. \tag{16}$$

2.2.3. Summary of the theory of diode biased linear PAs

If the diode bias branch can be omitted in the AC analysis, Equation (16) indicates that the size of the diode has no effect on the linearity of the linear PA. Comparing Eq. (16) with Eq. (9), the offset of I_0 as a function of an increase in $v_{\rm sm}$ for the diode biased PA is approximately half that for a regular current biased PA. So, the linearity of the former diode-biased PA is better, which is the theoretical foundation of Ref. [5]. A more precise relationship between IMR3/I_0 and $v_{\rm sm}$ can be simulated by MATLAB. Since the DC current I_0 decreases

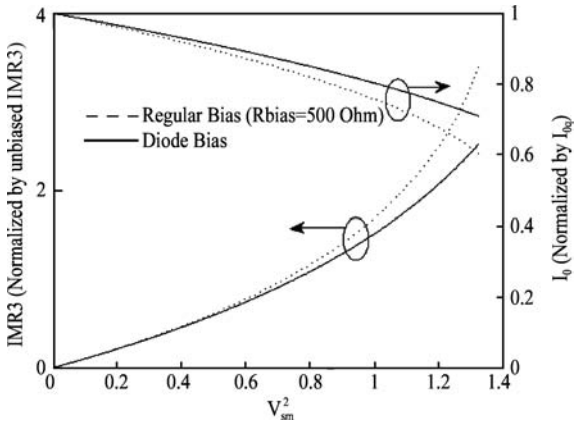

Fig. 7. AC-influencing DC current I_0 and IMR3 (normalized) in different bias PA.

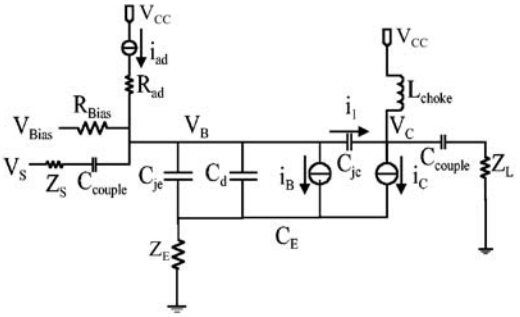

Fig. 8. Principle equivalent circuit of the proposed adaptive-biased PA.

more slowly in a diode biased PA, IMR3 is up to 3 dB better than for a regular bias ($R_{\rm Bias}$ = 500 Ω) when the input increases, as Figure 7 shows.

Actually, the leakage problem still exists due to the parasitic capacitance of the BE junction capacitance of the bias diode. Besides, the temperature coefficient of the DC current is larger than for a regular biased PA, which can be calculated to be (ignoring the temperature coefficient of $I_{\rm s}$)

$$\frac{\partial I_{0\rm q}}{\partial T} = -\frac{\ln\dfrac{I_{0\rm q}}{I_{\rm s}} + \ln\dfrac{I_{0\rm q}}{(1+\beta)\,I_{\rm s0}}}{2}\frac{I_{0q}}{T}. \tag{17}$$

Comparing Eq. (17) with Eq. (12), the temperature coefficient of the diode biased PA is almost ($\frac{I_{0\rm q}R_{\rm Bias}}{V_{\rm T}\beta}$ + 1) times the temperature coefficient of the regular biased PA, which has a negative impact on the temperature-correlative robustness of PA.

3. Adaptive bias to improve the linearity

3.1. Principal idea to improve the linearity

From the comparative results of the aforementioned two bias types, it was shown that the diode bias can improve the linearity by decreasing the drop of the DC current I_0. So, if an adaptive bias can completely compensate the drop, the linearity can be further improved. Figure 8 shows a principle equivalent circuit of an adaptive-biased PA. To reduce the leakage from the bias branches, the bias resistance can be large ($R_{\rm ad}, R_{\rm Bias} \gg \beta R_{\rm e}$), so that the AC analysis is the same as for Eqs. (4) and (5), while the DC equation is

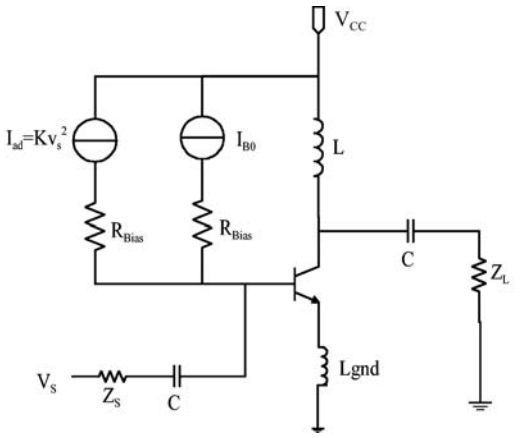

Fig. 9. Simulation schematic of the proposed adaptive-bias linear PA.

$$V_{\rm T}\ln\frac{I_0}{I_{\rm s}} + R_{\rm Bias}\left(\frac{I_0 + i_{\rm c}|_{\rm DC}}{\beta} - i_{\rm ad}\right) - V_{\rm Bias} = 0. \tag{18}$$

The adaptive bias $i_{\rm ad}$ satisfies the following equation,

$$i_{\rm ad} = \frac{i_{\rm c}|_{\rm DC}}{\beta} = \frac{I_0\,|C_1(s)|^2}{4\beta}v_{\rm sm}^2. \tag{19}$$

The DC voltage $v_{\rm be}|_{\rm DC}$ and the DC current I_0 will not be affected by $v_{\rm sm}$. So, the linearity could be improved.

3.2. Simulation for validation

The schematic used for the ADS simulation of the proposed adaptive-bias linear PA is shown in Fig. 9. For simplicity in the simulation. the voltage source $V_{\rm Bias}$ can be replaced by a current source $I_{\rm Bias}$. The adaptive DC current bias $I_{\rm ad}$ is proportional to the input AC power,

$$I_{\rm ad} = k_1 v_{\rm s}^2. \tag{20}$$

A harmonic balance (HB) simulation is carried out with sweeping k_1 from 0 to $k_{\rm opt} = \frac{I_{\rm B0}|C_1(s)|^2}{4}$. Figure 10 shows the relationship between the DC bias voltage/current and the input power. The figures indicate that the DC bias voltage/current drops rapidly without the adaptive bias (k_1 = 0). The output power and the AM-AM/AM-PM nonlinearity is shown in Fig. 11. We can see that the adaptive bias could enhance the maximum linear output power (1-dB compression power $P_{\rm 1dB}$) by 5 dB, and the AM-PM is substantially improved. An interesting result from Fig. 12 is that, although the PAE of the adaptive bias PA is lower, the PAE at $P_{\rm 1dB}$ can be increased from 20% to 32% when increasing $P_{\rm 1dB}$.

3.3. Implementation and test results

The circuit in Ref. [10] can realize the AC-to-DC relationship indicated by Eq. (20). A two-stage adaptive PA is fabricated in a Jazz 0.35-μm SiGe HBT process. Figure 13 shows the PA test board. The working frequency is 1.95 GHz. The test results are shown in Fig. 14: the 2-dB compression point and 3-dB compression point can be improved by 1.6 and 3.6 dB, respectively, which shows that the proposed adaptive bias PA brings an improvement.

Traditionally an adaptive bias is used to enhance the efficiency at lower output. To our knowledge there is no paper on the adaptive bias giving a theoretical analysis and suggesting

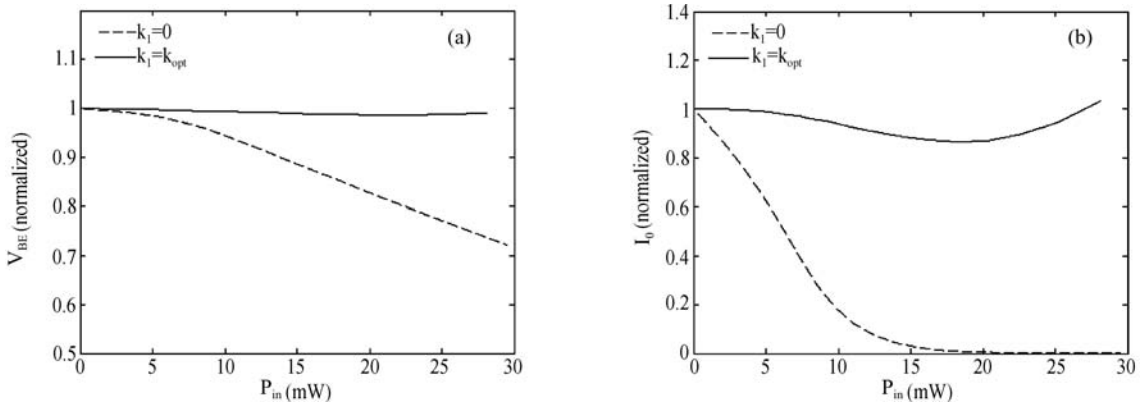

Fig. 10. Simulated (a) DC bias voltage V_{BE} and (b) DC current I_0 (normalized) of different bias PAs.

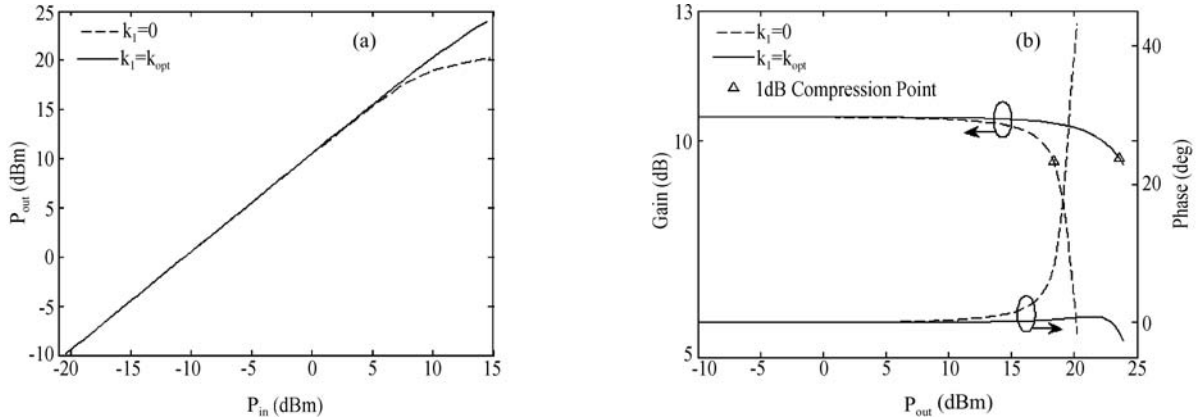

Fig. 11. Simulated (a) Output power and (b) AM-AM/AM/PM of different bias PAs.

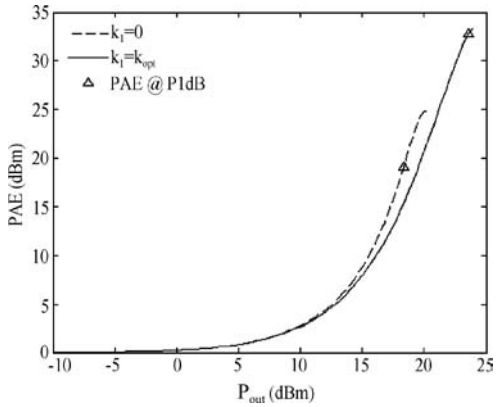

Fig. 12. Simulated power-added efficiency of different bias PAs.

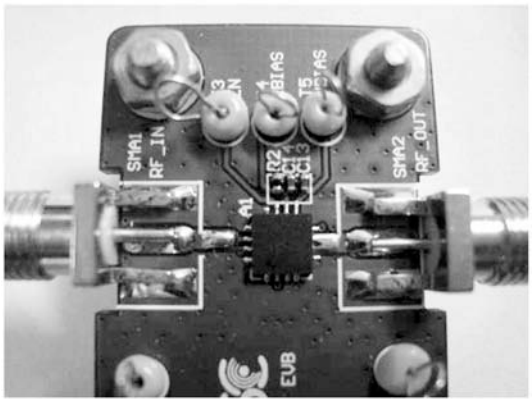

Fig. 13. Test board of the fabricated PA.

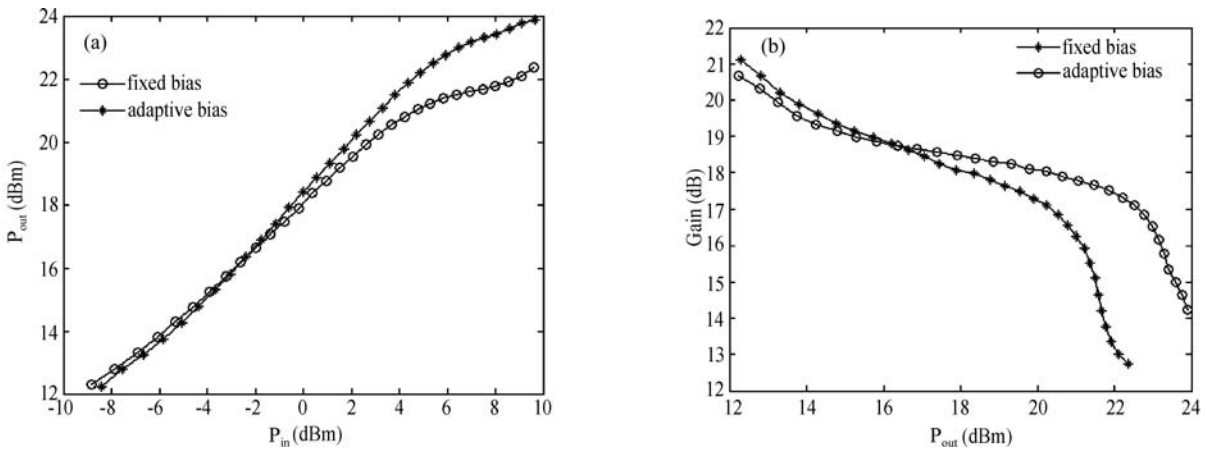

Fig. 14. Test results of different biased PAs: (a) Output power; (b) Gain.

further improvements. Deduction, simulation, and test validation in this paper demonstrates that the adaptive bias current, which satisfied Eq. (17), can effectively enhance the linear output power without impairing the efficiency by decreasing the drop of the DC current I_0. Besides, the adaptive current bias can reduce the temperature coefficient because V_T does not affect the bias current.

4. Conclusion

In this paper, a detailed analysis of the DC bias of linear PAs and the relationship between the linearity and the bias is given. An adaptive bias prototype is proposed to improve the linearity without impairing the efficiency. This prototype is validated by MATLAB/ADS simulations and test results.

Appendix

Deduction for Eq. (4):

According to Fig. 2, the AC equation is

$$i_1 = sC_{jc}\left[v_{be} + \left(i_c + i_b + sC_{je}v_{be} + s\tau i_c\right)Z_e - (i_1 - i_c)Z_L\right]. \tag{A1}$$

So

$$i_1 = \frac{sC_{jc}\left[v_{be} + (i_c + i_b)Z_e + sC_{je}v_{be}Z_e + s\tau i_c Z_e + i_c Z_L\right]}{1 + sC_{jc}Z_L}. \tag{A2}$$

Then

$$\begin{aligned} i_s &= sC_{je}v_{be} + s\tau i_c + i_b + i_1 \\ &= A_1(s)\left(\frac{v_{be}}{V_T}\right) + A_2(s)\left(\frac{v_{be}}{V_T}\right)^2 + A_3(s)\left(\frac{v_{be}}{V_T}\right)^3, \end{aligned} \tag{A3}$$

where

$$\begin{aligned} A_1(s) &= I_0\left(\frac{1}{\beta} + s\tau\right) + sC_{je}V_T \\ &+ \frac{sC_{jc}}{1 + sC_{jc}Z_L}\left[\left(1 + sC_{je}Z_e\right)V_T + I_0\left(1 + \frac{1}{\beta} + s\tau\right)Z_e + I_0 Z_L\right], \\ A_2(s) &= \frac{I_0}{2}\left\{\frac{1}{\beta} + s\tau + \frac{sC_{jc}}{1 + sC_{jc}Z_L}\left[Z_L + \left(1 + \frac{1}{\beta} + s\tau\right)Z_e\right]\right\}, \\ A_3(s) &= \frac{I_0}{6}\left\{\frac{1}{\beta} + s\tau + \frac{sC_{jc}}{1 + sC_{jc}Z_L}\left[Z_L + \left(1 + \frac{1}{\beta} + s\tau\right)Z_e\right]\right\}. \end{aligned}$$

Substituting into $v_s = i_s Z_s + v_{be} + \left(i_c + i_b + sC_{je}v_{be} + s\tau i_c\right)Z_e$, we get Eq. (4).

Deduction for Eq. (6):

In Fig. 2, the DC equation can be written as follows (normally $R_e \ll \frac{R_{Bias}}{\beta}$):

$$V_{BE} + \frac{R_{BIAS}}{\beta}\left(I_0 + i_c|_{DC}\right) - V_{Bias} = 0. \tag{A4}$$

The collector AC current is approximately

$$i_c = I_0\left[\frac{v_{be}}{V_T} + \frac{1}{2}\left(\frac{v_{be}}{V_T}\right)^2 + \frac{1}{6}\left(\frac{v_{be}}{V_T}\right)^3\right] \tag{A5}$$

when

$$v_s = v_{sm}\cos\omega t = \frac{1}{2}\left(e^{st} + e^{-st}\right).$$

Considering Eq. (5) and Volterra's theory[9],

$$i_c|_{DC} = \frac{v_{sm}^2}{4} I_0 C_1(s) C_1(-s), \tag{A6}$$

so we get Eq. (6).

Deduction for Eq. (11):

$$i_{out} = i_c - i_1 = E_1(s)\frac{v_{be}}{V_T} + E_2(s)\left(\frac{v_{be}}{V_T}\right)^2 + E_3(s)\left(\frac{v_{be}}{V_T}\right)^3, \tag{A7}$$

where

$$\begin{aligned} E_1(s) &= I_0 - \frac{sC_{jc}}{1 + sC_{jc}Z_L}\left[\left(1 + sC_{je}Z_e\right)V_T \right. \\ &\left. + I_0\left(1 + \frac{1}{\beta} + s\tau\right)Z_e + I_0 Z_L\right], \\ E_2(s) &= \frac{I_0}{2}\left\{1 - \frac{sC_{jc}}{1 + sC_{jc}Z_L}\left[Z_L + \left(1 + \frac{1}{\beta} + s\tau\right)Z_e\right]\right\}, \\ E_3(s) &= \frac{I_0}{6}\left\{1 - \frac{sC_{jc}}{1 + sC_{jc}Z_L}\left[Z_L + \left(1 + \frac{1}{\beta} + s\tau\right)Z_e\right]\right\}. \end{aligned}$$

Combining with Eq. (5),

$$i_{out} = F_1(s)v_s + F_2(s_1, s_2)v_s^2 + F_3(s_1, s_2, s_3)v_s^3, \tag{A8}$$

where

$$\begin{aligned} F_1(s) &= E_1(s)C_1(s), \\ F_2(s_1, s_2) &= E_1(s_1 + s_2)C_2(s_1, s_2) + E_2(s_1 + s_2)C_1(s_1)C_1(s_2), \\ F_3(s_1, s_2, s_3) &= E_1(s_1 + s_2 + s_3)C_3(s_1, s_2, s_3) \\ &+ E_3(s_1 + s_2 + s_3)C_1(s_1)C_1(s_2)C_1(s_3) \\ &+ 2E_2(s_1 + s_2 + s_3)\overline{C_1C_2}. \end{aligned}$$

2-tone:

$$\begin{aligned} v_s &= \frac{v_{sm}}{\sqrt{2}}(\cos\omega_1 t + \cos\omega_2 t) = \frac{v_{sm}}{2\sqrt{2}}\left(e^{s_1 t} + e^{-s_1 t} + e^{s_2 t} + e^{-s_2 t}\right) \\ |\mathrm{IMR3}| &= \left|\frac{3}{4}\frac{F_3(s_1, s_1, -s_2)}{F_1(s_1)}\right|\left|\frac{v_{sm}}{\sqrt{2}}\right|^2 \\ &= \frac{3|v_{sm}|^2}{8}\left|C_1(s)C_1(-s)\left[\frac{E_3(s)}{E_1(s)} - C_1(s)B_3(s)\right]\right. \\ &\left. + 2C_1(s)C_1(-s)\overline{B_2C_1}\left[C_1(s)B_2(s) - \frac{E_2(s0)}{E_1(s)}\right]\right| \\ &= \frac{3|v_{sm}|^2}{8}|C_1(s)|^2\left|\frac{E_3(s)}{E_1(s)} - C_1(s)B_3(s)\right. \\ &\left. + 2\overline{B_2C_1}\left[C_1(s)B_2(s) - \frac{E_2(s)}{E_1(s)}\right]\right|, \end{aligned} \tag{A9}$$

so we get Eq. (11).

References

[1] Burr A. Modulation and coding for wireless communications. Beijing: Publishing House of Electronics Industry, 2003

[2] Vuolevi J, Rahkonen T. The effects of source impedance on the linearity of BJT common-emitter amplifiers. Proceedings of the International Symposium on Circuits and Systems, 2000, 4: IV197

[3] Cripps S C. RF power amplifiers for wireless communications. Norwood: Artech House Inc, 1999

[4] De Carvalho N B, Pedro J C. Large- and small-signal IMD behavior of microwave power amplifiers. IEEE Trans Microw Theory Tech, 1999, 47: 2364

[5] Youn S N, Chul S P. PCS/W-CDMA dual-band MMIC power amplifier with a newly proposed linearizing bias circuit. IEEE J Solid-State Circuits, 2002, 37: 1096

[6] Yang Y, Choi K, Weller K P. DC boosting effect of active bias circuits and its optimization for class-AB InGaP-GaAs HBT power amplifiers. IEEE Trans Microw Theory Tech, 2004, 52: 1455

[7] Schetzen M. The Volterra and Wiener theories of nonlinear systems. New York: John Wiley & Sons, 1980

[8] Fong K L, Meyer R G. High-frequency nonlinearity analysis of common-emitter and differential-pair transconductance stages. IEEE J Solid-State Circuits, 1998, 33: 548

[9] Wambacq P. Distortion analysis of analog integrated circuits. Boston: Kluwer Academic Publishers, 1998

[10] Zhang T, Eisenstadt W R, Fox R M. A novel 5 GHz RF power detector. Proceedings of the International Symposium on Circuits and Systems, 2004